J. Phys. Chem. A **2006,** *110,* 4833−4838

An Investigation of Hydrogen-Bonding Effects on the Nitrogen and Hydrogen Electric Field Gradient and Chemical Shielding Tensors in the 9-Methyladenine Real Crystalline Structure: A Density Functional Theory Study

Mahmoud Mirzaei and Nasser L. Hadipour*

Department of Chemistry, Tarbiat Modares University, P.O. Box 14115-175, Tehran, Iran

Received: January 5, 2006; In Final Form: February 13, 2006

Hydrogen-bonding effects in the real crystalline structure of 9-methyladenine, 9-MA, were studied using calculated electric field gradient, EFG, and chemical shielding, CS, tensors for nitrogen and hydrogen nuclei via density functional theory. The calculations were carried out at the B3LYP and B3PW91 levels with the 6-311++G** basis set via the Gaussian 98 package. Nuclear quadrupole coupling constants, C_Q, and asymmetry parameters, η_Q, are reported for ^{14}N and ^{2}H. The chemical shielding anisotropy, $\Delta\sigma$, and chemical shielding isotropy, σ_{iso}, are also reported for ^{15}N and ^{1}H. The difference between the calculated parameters of the monomer and heptameric layer-like cluster 9-MA shows how much H-bonding interactions affect the EFG and CS tensors of each nucleus. This result indicates that N(10) (imino nitrogen) has a major role in H-bonding interactions, whereas that of N(9) is negligible. There is good agreement between the present calculated parameters and reported experimental data. Although some discrepancies were observed, this could be attributed to the different conditions which were applied for calculation and the experiments.

Introduction

It is well-known that hydrogen-bonding interactions play a key role in both chemical and biochemical systems. Watson and Crick in a pioneering work indicated the importance of H-bonding interactions between tautomeric A−T and G−C base pairs in the stabilization of the nucleic acid secondary structure.[1] Indeed, knowing the circumstances of the base pairing interactions may be a crucial step to understand the conformation, activity, and 3D structure of biomolecules.[2] H-bonding effects on the properties of nucleobases in biomolecules have been recognized.[3,4]

It is an interesting subject to investigate H-bonding interactions in adenine, 6-aminopurine, and its derivatives because of their multiple roles as nucleic acid building blocks, energy storage systems, and reaction catalysts in biosystems.[5] Numerous studies in various experimental and theoretical fields have been devoted to characterize these H-bonding interactions in both adenine and its derivatives.[6−8]

Nuclear magnetic resonance, NMR, spectroscopy including static and magic angle spinning, MAS, is one of the most efficient techniques to study the nature of H-bonds.[9−14] NMR studies in both the solution and solid phases have been reported for magnetically active nuclei, e.g., ^{1}H and ^{15}N, in adenine derivatives.[15−19] By solid-state NMR the principal values of chemical shielding, CS, and electric field gradient, EFG, tensors can be measured, which provide information about intermolecular interactions, e.g., H-bonding. The CS tensors are strongly influenced by the H-bond length. Although this influence can be studied experimentally on the isotropic CS tensors of ^{1}H and ^{15}N, on the other hand it cannot be studied on the anisotropic CS tensors of these nuclei in a systematic way, and the theoretical approaches are just evidence for this purpose.[20] H-bonding interactions also cause changes in the EFG tensors of resonating quadrupole nuclei, e.g., ^{2}H and ^{14}N. The electric quadrupole moment, eQ, interacts with the EFG tensors which arise from the internal electrostatic charges at the site of each quadrupole nucleus.[21] Especially, the technique of nuclear quadrupole resonance, NQR, spectroscopy is employed to indicate the changes in EFG tensors, which are reflected in the observed shift of the NQR spectrum.[22] NQR studies for adenine derivatives have also been reported.[23]

9-Methyladenine, 9-MA, is an adenine derivative where a methyl group is substituted for H(9); see Chart 1. 9-MA has been chosen to be studied in the present work for several reasons. First, the site of adenine which binds with the sugar group, e.g., in adenosine, is N(9), and because of bonding similarity between N(9)−CH_3 and N(9)−sugar, 9-MA becomes an important model which can be considered to investigate the properties of N(9)−group adenine derivatives.[24] Second, the accurate crystalline structure of 9-MA by neutron diffraction study is available.[25] Third, it was exhibited in the crystalline structure that there is an unusual H-bond as C−H···N, so it is interesting to characterize the properties of this H-bond by the EFG and CS results. Fourth, to the best of our knowledge there is a lack of NMR and NQR data to characterize the nitrogen and hydrogen nuclei in 9-MA, so it is a good idea to do this by the theoretical calculations performed on the real crystalline structure.

In most theoretical studies just a single computationally drawn molecule is calculated, so a discrepancy between theoretical and experimental results is expected. Previously, it was reported that if a molecule is considered in its real crystalline structure, the results are more reliable and closer to the experimental results.[26−30] In this study, 9-MA is also considered as the central molecule in a heptameric cluster, so the effects of neighbor molecules are included as close to the real crystalline structure as possible. EFG and CS tensors in their principal axis system,

---

* To whom correspondence should be addressed. E-mail: hadipour@modares.ac.ir and hadipour_n@yahoo.com.

10.1021/jp0600920 CCC: $33.50

CHART 1: (a) Adenine, (b) 9-Methyladenine, (c) Heptameric Layer-like Cluster of 9-MA, and (d) Intermolecular H-Bonding Interactions in Cluster 9-MA[a]

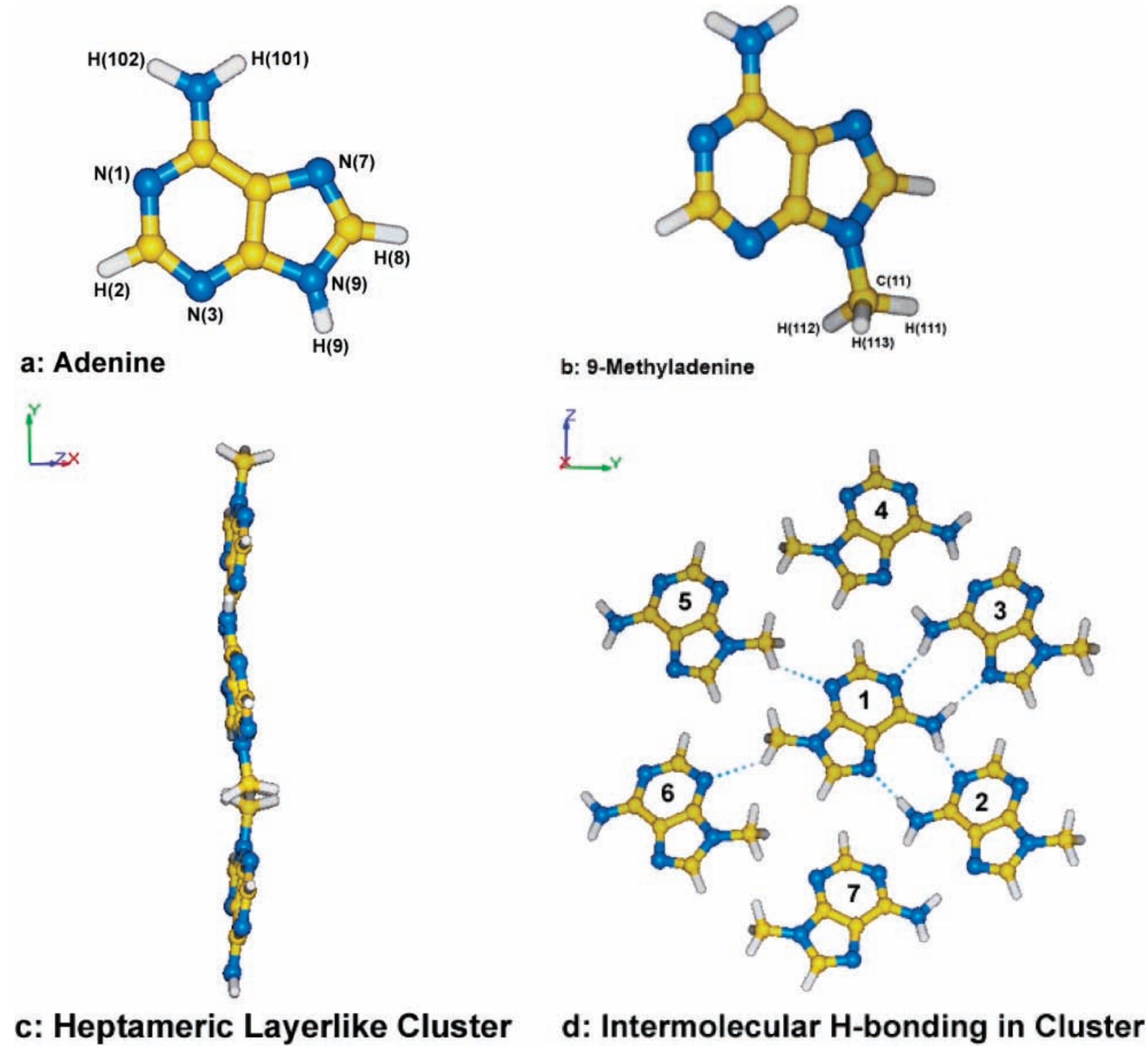

[a] See Table 1 for details.

PAS, for nitrogen and hydrogen nuclei are calculated using density functional theory, DFT. The calculated EFG tensors are reported as nuclear quadrupole coupling constants, C_Q, and asymmetry parameters, η_Q, in Tables 2 and 3. The calculated CS tensors are reported as chemical shielding principal components, σ_{ii}, chemical shielding isotropy, σ_{iso}, and chemical shielding anisotropy, $\Delta\sigma$, in Tables 4 and 5.

Computational Aspects

All the computational calculations were performed using DFT with the Gaussian 98W package.[31] Since the crystalline structure of 9-MA was obtained from a neutron diffraction study, geometry optimization was not needed in this work. B3LYP and B3PW91[32-34] are the two levels of the method and 6-311++G** is the standard basis set which are reliable to calculate the nitrogen and hydrogen EFG and CS tensors in the PAS.[29,30,35,36] The gauge-included atomic orbital, GIAO, approach[37] was used in the CS tensor calculations. The principal CS tensor eigenvalues, σ_{11}, σ_{22}, and σ_{33}, have the following relation: $\sigma_{33} > \sigma_{22} > \sigma_{11}$. Chemical shielding anisotropy, $\Delta\sigma$, is obtained by $\Delta\sigma = \sigma_{33} - (\sigma_{22} + \sigma_{11})/2$ (ppm). Chemical shielding isotropy, σ_{iso}, is obtained by $\sigma_{iso} = (\sigma_{11} + \sigma_{22} + \sigma_{33})/3$. To convert ^{15}N σ_{iso} to chemical shift isotropy, δ_{iso}, nitromethane with a σ_{iso} of -135.8 ppm was chosen as the reference,[38] $\delta_{iso} = \sigma_{iso,r} - \sigma_{iso,s}$, where the subscripts "r" and "s" refer to the reference and sample, respectively.

The principal EFG tensor eigenvalues, q_{zz}, q_{yy}, and q_{xx}, have the following relation: $|q_{zz}| > |q_{yy}| > |q_{xx}|$. The nuclear quadrupole coupling constant, C_Q, is obtained by $C_Q = e^2q_{zz}Q/h$ (MHz). Q values of ^{14}N and ^{2}H, which are used in the calculation of C_Q values, have been reported by Pyykkö as 20.44 and 2.56 mb, respectively.[39] Another important parameter which refers to the deviation of charge distribution from cylindrical symmetry is the asymmetry parameter, η_Q: $\eta_Q = |(q_{xx} - q_{yy})/q_{zz}|$.

It is noteworthy that a heptameric layer-like cluster of 9-MA, see Chart 1, was created using neutron diffraction coordinates and considered in the calculations. Although the calculations

TABLE 1: Distances (Å) between Interactive N and H of 9-MA in the Cluster[a]

r[central···neighbor][b]	
r[N(1)···H(101-3: $x, ^1/_2 - y, ^1/_2 + z$)]	1.96
r[N(3)···H(111-5: $x, -^1/_2 - y, ^1/_2 + z$)]	2.52
r[N(7)···H(102-2: $x; ^1/_2 - y, -^1/_2 + z$)]	2.04
r[N(10)···N(1-2: $x, ^1/_2 - y, -^1/_2 + z$)]	2.96
r[N(10)···N(7-3: $x, ^1/_2 - y, ^1/_2 + z$)]	3.05
r[H(2)···H(8-4: $x, y, 1 + z$)]	2.48
r[H(8)···H(2-7: $x, y, -1 + z$)]	2.48
r[H(101)···N(1-2: $x, ^1/_2 - y, -^1/_2 + z$)]	1.96
r[H(102)···N(7-3: $x, ^1/_2 - y, ^1/_2 + z$)]	2.04
r[H(111)···N(3-6: $x, -^1/_2 - y; -^1/_2 + z$)]	2.52
r[H(113)···H(8-5: $x, -^1/_2 - \mathrm{y}, ^1/_2 + z$)]	2.68

[a] The experimental data are from ref 25. [b] H(101-3: $x, ^1/_2 - y, ^1/_2 + z$) denotes H(101) of molecule number 3 with the transformation $x, ^1/_2 - y, ^1/_2 + z$.

were performed for the whole cluster, the parameters for the central molecule and their changes in the intermolecular H-bonding interactions were considered and are reported.

Another calculation was also performed for a fully optimized isolated gas-phase 9-MA to calculate the EFG and CS tensors. The full geometry optimization was carried out at the B3LYP level with 6-311++G**.

Results and Discussion

In the present work, including intermolecular H-bonding interactions, 9-MA was considered in a heptameric layer-like cluster; see Chart 1. As mentioned earlier, 9-MA structural optimization was not needed. The distances between the central 9-MA nitrogen and hydrogen and those of the first neighbors in the same layer are listed in Table 1. To indicate the influence of H-bonding interactions on the NMR parameters of various nuclei, the calculated parameters were compared between the cluster and fully optimized isolated gas-phase 9-MA. In the following, the results of the calculations will be discussed in two parts separately.

Electric Field Gradient Tensors. In this part, the DFT calculations at the B3LYP and B3PW91 levels were carried out to investigate the effect of H-bonding interactions on the ^{14}N and ^{2}H EFG tensors of 9-MA. To make a direct relation between the calculated EFG tensors and C_Q and η_Q, which are observed experimentally, their equations mentioned in the Computational Aspects were used. The nuclear quadrupole coupling constants, C_Q, and asymmetry parameters, η_Q, for ^{14}N and ^{2}H are summarized in Tables 2 and 3.

By a quick look at the results, one can easily obtain some trends. First, the C_Q values of those nuclei which participate in the intermolecular H-bonding interactions decrease, but on the other hand, their η_Q values increase from the isolated gas phase to the cluster. The magnitude of these changes for each nucleus depends on its contribution to the interactions. Second, the calculated parameters of B3LYP and B3PW91 are practically contiguous with each other. In the following text B3LYP results are referred to.

From Table 2 it is obvious that, with the exception of N(9), the other four nitrogens are affected by H-bonding interactions. N(10) with a remarkable $\Delta C_Q(^{14}\mathrm{N})$ of 1.5 MHz and a $\Delta\eta_Q$ of 0.36 is the most affected nucleus of 9-MA in the H-bonding interactions. Because H(101) and H(102) have proper distances of H-bonds, *r*[H(101)···N(1-2)] = 1.96 Å and *r*[H(102)···N(7-3)] = 2.04 Å, they also have remarkable changes among the hydrogens; see Table 3. They have $\Delta C_Q(^2\mathrm{H})$ values of 61 and 52 kHz and $\Delta\eta_Q$ values of 0.03 and 0.02, respectively.

TABLE 2: Calculated and Experimental EFG Tensors of ^{14}N

	C_Q[a] (MHz)			η_Q[a]		
nucleus	isolated gas phase[b]	cluster[c]	exptl[d]	isolated gas phase[b]	cluster[c]	exptl[d]
N(1)	4.19	3.85	3.407	0.182	0.318	0.335
	(4.12)	(3.75)		(0.199)	(0.343)	
N(3)	4.05	3.74	3.883	0.124	0.255	0.188
	(3.98)	(3.65)		(0.143)	(0.277)	
N(7)	4.05	3.78	3.203	0.083	0.174	0.215
	(3.96)	(3.67)		(0.106)	(0.202)	
N(9)	3.33	3.07	1.990	0.184	0.163	0.688
	(3.29)	(3.04)		(0.193)	(0.172)	
N(10)	4.73	3.24	2.843	0.121	0.485	0.468
	(4.65)	(3.22)		(0.127)	(0.484)	

[a] The calculated results not in parentheses are from B3LYP, and those in parentheses are from B3PW91. [b] Fully optimized isolated gas-phase 9-MA. [c] Target molecule in the cluster. [d] The experimental data are from ref 23.

TABLE 3: Calculated EFG Tensors of ^{2}H

	C_Q[a] (kHz)		η_Q[a]	
nucleus	isolated gas phase[b]	cluster[c]	isolated gas phase[b]	cluster[c]
H(2)	209.0	202.3	0.058	0.076
	(210.0)	(203.3)	(0.057)	(0.073)
H(8)	216.1	217.3	0.095	0.102
	(217.3)	(218.4)	(0.093)	(0.100)
H(101)	279.4	218.8	0.188	0.218
	(281.0)	(219.8)	(0.186)	(0.214)
H(102)	280.4	228.8	0.177	0.198
	(281.8)	(229.9)	(0.175)	(0.195)
H(111)	203.5	212.6	0.084	0.062
	(204.5)	(213.8)	(0.083)	(0.061)
H(112)	200.7	208.4	0.071	0.073
	(201.6)	(209.4)	(0.071)	(0.073)
H(113)	200.1	206.6	0.074	0.073
	(201.1)	(207.7)	(0.074)	(0.073)

[a] The calculated results not in parentheses are from B3LYP, and those in parentheses are from B3PW91. [b] Fully optimized isolated gas-phase 9-MA. [c] Target molecule in the cluster.

The mentioned results indicate the importance of the $-NH_2$ group in 9-MA H-bonding interactions.

N(1), *r*[N(1)···H(101-3)] = 1.96 Å, with a $\Delta C_Q(^{14}\mathrm{N})$ of 0.34 MHz and a $\Delta\eta_Q$ of 0.14 is the next affected nucleus of 9-MA in the H-bonding interactions. $\Delta C_Q(^{14}\mathrm{N})$ = 0.27 MHz and $\Delta\eta_Q$ = 0.09 belong to N(7), *r*[N(7)···H(102-2)] = 2.04 Å, which is the next affected nucleus. Placing N(1) in the six-membered ring but N(7) in the five-membered ring and also the smaller H-bond distance of N(1) may cause the different changes in their $C_Q(^{14}\mathrm{N})$ and η_Q values.

N(3) is located toward the methyl group of N(9-5). H(111-5) is the H of $-CH_3$ which is in the same layer with a distance of *r*[N(3)···H(111-5)] = 2.52 Å from the central 9-MA. Although this distance is larger than those mentioned so far for the H-bonding interactions, it is still smaller than the van der Waals interaction distance so it is expected as a H-bond, which is more transparent from Tables 2 and 3. In these tables, $\Delta C_Q(^{14}\mathrm{N})$ = 0.31 MHz for N(3) and $\Delta C_Q(^2\mathrm{H})$ = 9.1 kHz for H(111) are observed. The $\Delta C_Q(^2\mathrm{H})$ of H(111) is smaller than those of H(101) and H(102), but it is the only hydrogen with which the neighboring N(3) can interact. For N(9), a reduction of 0.02 in η_Q indicates its negligible role in making H-bonds.

As mentioned above, H-bonding interactions have different influences on various nuclei in the 9-MA cluster. Considering a complete set of 9-MA molecules is an advantage of NMR

TABLE 4: Calculated and Experimental CS Tensors of ^{15}N

		$\sigma_{ii}{}^{a}$ (ppm)		$\sigma_{iso}{}^{a}$ (ppm)		$\Delta\sigma^{a}$ (ppm)		δ_{iso} (ppm)	
nucleus	σ_{ii}	isolated gas phase[b]	cluster[c]	isolated gas phase[b]	cluster[c]	isolated gas phase[b]	cluster[c]	cluster[a,d]	exptl[e]
N(1)	σ_{11}	−171.4 (−166.1)	−147.4 (−140.4)	−6.60 (−1.34)	−0.71 (4.69)	367.9 (369.2)	340.4 (339.5)	−135.1 (−140.5)	−158
	σ_{22}	−87.6 (−82.7)	−80.9 (−76.6)						
	σ_{33}	238.6 (244.8)	226.2 (230.9)						
N(3)	σ_{11}	−169.4 (−165.9)	−143.3 (−138.8)	2.34 (7.09)	13.8 (18.7)	394.8 (394.5)	368.9 (367.8)	−149.6 (−154.5)	−167
	σ_{22}	−89.2 (−82.9)	−75.1 (−69.0)						
	σ_{33}	265.5 (270.1)	259.8 (263.9)						
N(7)	σ_{11}	−217.3 (−211.9)	−205.1 (−198.1)	−12.8 (−7.54)	−14.3 (−8.43)	386.4 (383.5)	361.5 (357.9)	−121.5 (−127.4)	−149
	σ_{22}	−65.8 (−58.8)	−64.5 (−57.4)						
	σ_{33}	244.8 (248.1)	226.6 (230.1)						
N(9)	σ_{11}	−6.75 (−1.25)	−74.4 (−2.0)	83.6 (87.3)	81.6 (85.4)	110.1 (108.4)	114.4 (112.7)	−217.4 (−221.2)	−221
	σ_{22}	100.5 (103.6)	94.3 (97.7)						
	σ_{33}	157.0 (159.6)	157.8 (160.5)						
N(10)	σ_{11}	119.1 (120.9)	74.3 (76.9)	174.6 (176.5)	142.5 (145.1)	82.6 (79.9)	59.8 (59.9)	−278.3 (−280.9)	−291
	σ_{22}	175.0 (178.8)	170.9 (173.3)						
	σ_{33}	229.6 (229.7)	182.4 (185.0)						

[a] The calculated results not in parentheses are from B3LYP, and those in parentheses are from B3PW91. [b] Fully optimized isolated gas-phase 9-MA. [c] Target molecule in the cluster. [d] The chemical shift isotropy of ^{15}N is obtained referred to nitromethane. [e] Experimental data are from ref 16.

parameter calculations. A similarity in the charge distributions of 9-MA and adenine was reported previously.[25] To exhibit this similarity, the calculated parameters were compared with the available experimental data of adenine trihydrate.[23] Because of the hydration, stronger influences of H-bonding interactions rather than those of 9-MA are observed in the parameters. However, the role of $-CH_3$ in the weaker H-bonding of 9-MA is not negligible.

Chemical Shielding Tensors. As mentioned in the previous part, the EFG tensors at the nitrogen and hydrogen nuclei are sensitive to the intermolecular H-bonding interactions. In this part, the effects of H-bonding interactions on the ^{15}N and ^{1}H CS tenors are discussed. To this aim, B3LYP and B3PW91 calculations were carried out for both forms of fully optimized isolated gas-phase and cluster 9-MA. The calculated CS tensors are reported as chemical shielding principal components, σ_{ii}, chemical shielding isotropy, σ_{iso}, and chemical shielding anisotropy, $\Delta\sigma$, in Tables 4 and 5.

Both B3LYP and B3PW91 calculations reveal that due to H-bonding interactions the nitrogen of the $-NH_2$ group is shielded 32 ppm in σ_{iso} and 22 ppm in $\Delta\sigma$ from isolated gas-phase to cluster 9-MA. In agreement with the EFG results, the changes in N(10) shielding values are also remarkable. The H-bond strength affects the NMR parameters of imino nitrogen. Because the distances of N(10) from two neighboring nitrogens in the same layer, N(1-2) and N(7-3), are 2.96 and 3.05 Å, respectively, there is a capability of making stronger H-bonds for H(101) and H(102) where their effects on N(10) parameters are observed. The results of H(101) and H(102) also have the main changes among the hydrogen nuclei of 9-MA. The parameters of N(1) and N(7) also change as a result of H-bonding interactions. They both interact with imino hydrogens, but because of having different distances, their parameter changes are also different. There are some notable discrepancies in the parameters of H(111); see Table 5. The discrepancies are because of the interaction between H(111) and N(3-6). With the exception of these two nuclei, there is no other chance for them to interact in the same layer. The changes of the N(3) parameters, $\Delta(\sigma_{iso}) = 12$ ppm and $\Delta(\Delta\sigma) = 26$ ppm, reveal the H-bonding interaction between H(111) and N(3-6), but it is weaker than that of N(10). These results are also observed for N(3) and H(111-5).

As mentioned in the Computational Aspects, in comparison with the experiment, the calculated isotropic chemical shieldings were converted to isotropic chemical shifts referring to nitromethane. The calculated ^{15}N parameters were compared with the available experimental data of adenine trihydrate;[16] see Table 4. The results of CS tensors are in good agreement with those of EFG tensors, which indicates the advantage of employing both of them in the interpretation of the influence of H-bonding interactions on various nuclei in the H-bonded systems.

Orientations of the EFG and CS Tensors. One important piece of information obtained by solid-state NMR is the relative orientations between the EFG and CS tensors. Performing high-level quantum chemical calculations also reveals reliable information about the orientation of the NMR tensors in the molecular frame. Previously, Brender and co-workers[35] reported the orientation of ^{15}N chemical shift tensors in peptides via quantum chemical calculations. A vast range of this kind of studies on ^{17}O NMR tensors, both experimentally and computationally, have also been reported by Wu and co-workers.[4,26,27,40−43]

TABLE 5: Calculated CS Tensors of ^1H

		σ_{ii}[a] (ppm)		σ_{iso}[a] (ppm)		$\Delta\sigma$[a] (ppm)	
nucleus	σ_{ii}	isolated gas phase[b]	cluster[c]	isolated gas phase[b]	cluster[c]	isolated gas phase[b]	cluster[c]
H(2)	σ_{11}	17.8	13.7	23.4	23.3	5.12	9.46
		(17.7)	(13.4)	(23.3)	(23.1)	(5.02)	(9.43)
	σ_{22}	25.6	26.6				
		(25.5)	(26.5)				
	σ_{33}	26.8	29.6				
		(26.7)	(29.4)				
H(8)	σ_{11}	20.3	16.2	24.5	24.1	4.65	7.30
		(20.1)	(16.0)	(24.4)	(24.0)	(4.67)	(7.27)
	σ_{22}	25.6	27.1				
		(25.6)	(27.1)				
	σ_{33}	27.6	28.9				
		(27.5)	(28.8)				
H(101)	σ_{11}	19.3	6.6	26.8	21.0	10.1	21.4
		(19.1)	(6.4)	(26.6)	(21.0)	(10.3)	(21.6)
	σ_{22}	27.5	21.2				
		(27.3)	(21.1)				
	σ_{33}	33.5	35.3				
		(33.5)	(35.4)				
H(102)	σ_{11}	21.7	7.7	27.3	21.6	11.0	20.9
		(21.5)	(7.7)	(27.2)	(21.6)	(11.3)	(21.1)
	σ_{22}	25.5	21.5				
		(25.3)	(21.4)				
	σ_{33}	34.6	35.5				
		(34.7)	(35.6)				
H(111)	σ_{11}	23.6	16.1	28.5	26.4	7.55	14.1
		(23.4)	(15.9)	(28.4)	(26.3)	(7.80)	(14.4)
	σ_{22}	28.4	27.3				
		(28.3)	(27.2)				
	σ_{33}	33.5	35.8				
		(33.6)	(35.9)				
H(112)	σ_{11}	24.2	21.7	28.4	28.0	9.75	9.82
		(24.1)	(21.5)	(28.3)	(27.9)	(9.94)	(9.95)
	σ_{22}	226.0	27.8				
		(25.9)	(27.7)				
	σ_{33}	34.9	34.5				
		(34.9)	(34.5)				
H(113)	σ_{11}	23.4	22.7	28.1	27.8	9.02	7.34
		(23.2)	(22.6)	(28.0)	(27.7)	(9.22)	(7.46)
	σ_{22}	26.8	27.9				
		(26.6)	(27.8)				
	σ_{33}	34.1	32.6				
		(34.2)	(32.6)				

[a] The calculated results not in parentheses are from B3LYP, and those in parentheses are from B3PW91. [b] Fully optimized isolated gas-phase 9-MA. [c] Target molecule in the cluster.

In the present study, the calculated relative orientations of nitrogen and hydrogen EFG and CS tensors were determined via B3LYP/6-311++G** for the target molecule in the heptameric cluster of 9-MA; see Table 6. From the results, it is indicated that for N(1), N(3), and N(7) q_{xx} and σ_{33} are almost perpendicular to the molecular plane. However, at N(1) these tensors have the reverse directions. Because of the different electron moieties, a discrepancy between the relative orientations of N(9) and N(10) and those of N(1) to (3) are observed. The largest components of the tensors, σ_{33} and q_{zz}, are in the same direction and almost perpendicular to the molecular plane at N(9). However, there is a 20° difference between σ_{33} and q_{zz} at N(10). The relative orientations of the EFG and CS tensors of H(101), H(102), and H(111) are almost similar. For the mentioned nuclei, the largest components of the tensors are in the same direction; however, a larger β (deg) is observed for H(111).

TABLE 6: Relative Orientations of the EFG and CS Tensors[a]

nucleus	α	β	γ
N(1)	177.8	89.1	69.0
N(3)	0.2	90.2	82.5
N(7)	1.4	89.9	79.4
N(9)	89.6	0.4	90.0
N(10)	93.8	20.4	93.7
H(2)	5.1	94.8	94.0
H(8)	175.4	93.5	85.3
H(101)	80.5	9.0	90.3
H(102)	94.0	4.9	87.0
H(111)	65.0	25.5	87.6
H(112)	129.0	39.0	57.3
H(113)	50.2	40.0	60.4

[a] The values are in degrees.

Conclusion

In this work, a computational solid-state nitrogen and hydrogen NMR study is reported for 9-MA. As observed from the results, both EFG and CS tensors of nitrogen and hydrogen are sensitive to H-bonding interactions. Therfore, to be sure of the calculated results, calculating both tensors is an advantage. The results of B3LYP and B3PW91 show good agreement in the parameter discrepancies from the isolated gas phase to the cluster. It is noteworthy that although the cross-layer effects are ignored in the considered layer-like cluster of 9-MA, the influence of H-bonding interactions on the calculated parameters are reasonably observed.

The results reveal that imino nitrogen and hydrogen are the most important nuclei of 9-MA in contributing to N−H···N H-bonding interactions. On the other hand, N(9) has almost no major role in making H-bonds. As a final note, the C−H···N type of H-bonding has an influence on the NMR parameters of N(3) and H(111), but it is weaker than that of the N−H···N type.

Acknowledgment. We gratefully thank Dr. Kamran Ahmadi for preparing the heptameric cluster of 9-MA and also Ms. Fatemeh Elmi, Ph.D candidate of our group, for her helpful guidance and discussions in preparing this manuscript.

References and Notes

(1) Watson, J.; Crick, H. C. *Nature* **1953**, *171*, 737.
(2) Sahu, P. K.; Mishra, R. K. and Lee, S-L. *J. Phys. Chem. A* **2005**, *109*, 2887.
(3) McConnell, T. L.; Wheaton, C. A.; Hunter, K. C. Wetmore, S. T. *J. Phys. Chem. A* **2005**, *109*, 6351.
(4) Wu, G.; Dong, S.; Ida, R.; Reen, N. *J. Am. Chem. Soc.* **2002**, *124*, 1768.
(5) Lewin, B. *Genes VI*; Oxford University Press: Oxford, U.K.; Cell Press: Cambridge, MA, 1997.
(6) Kryachko, E. S.; Sabin, J. R. *Int. J. Quantum Chem.* **2003**, *91*, 695.
(7) Kawahara, S.-I.; Uchimaru, T.; Taira, K. and Sekine, M. *J. Phys. Chem. A* **2001**, *105*, 3894.
(8) Hobza, P.; Sponer, J.; Cubero, E.; Orozco, M.; Luque, F. J. *J. Phys. Chem. B* **2000**, *104*, 6286.
(9) Wei, Y.; de Dios, A. C.; McDermott, A. E. *J. Am. Chem. Soc.* **1999**, *121*, 10389.
(10) Sack, I.; Macholl, S. *Appl. Magn. Reson.* **1999**, *17*, 413.
(11) Lee, D.-K.; Ramamoorthy, A. *J. Magn. Reson.* **1998**, *113*, 204.
(12) Liwang, A. C.; Bax, A. *J. Magn. Reson.* **1997**, *127*, 54.
(13) Gu, Z.; Ridenour, C. F. *J. Am. Chem. Soc.* **1996**, *118*, 822.
(14) Michal, C. A.; Wehman, J. C.; Jelinski, L. W. *J. Magn. Reson., Ser. B* **1996**, *111*, 31.
(15) Major, D. T.; Laxer, A.; Fischer, B. *J. Org. Chem.* **2002**, *67*, 790.
(16) Hu, J. Z.; Facelli, J. C.; Alderman, D. W.; Pugmire, R. J.; Grant, D. M. *J. Am. Chem. Soc.* **1998**, *120*, 9863.
(17) Gaffney, B. L.; Kung, P.-P.; Wang, C.; Jones, R. A. *J. Am. Chem. Soc.* **1995**, *117*, 12281.

(18) Schindler, M. *J. Am. Chem. Soc.* **1988**, *110*, 6623.

(19) Charland, J.-P.; Viet, M. T. P.; St-Jacques, M.; Beauchamp, A. L. *J. Am. Chem. Soc.* **1985**, *107*, 8202.

(20) Czernek, J.; Fiala, R.; Sklenáø, V. *J. Magn. Reson.* **2000**, *145*, 142.

(21) Cohen, M. H.; Rief, F. *Solid State Phys.* **1957**, *5*, 321.

(22) Das, T. P.; Han, E. L. *Nuclear Quadrupole Resonance Spectroscopy*; Academic Press: New York, 1958.

(23) Rabbani, S. R.; Edmonds, D. T.; Gosling, P. *J. Magn. Reson.* **1987**, *72*, 422.

(24) Wiorkiewicz-Kuczera, J.; Karplus M. *J. Am. Chem. Soc.* **1990**, *112*, 5324.

(25) McMullan, R. k.; Benci, P.; Craven, B. M. *Acta Crystallogr., Sect. B* **1980**, *36*, 1424.

(26) Ida, R.; Clerk, M. D.; Wu, G. *J. Phys. Chem. A* **2006**, *110*, 1065.

(27) Dong, S.; Ida, R.; Wu, G. *J. Phys. Chem. A* **2000**, *104*, 11194.

(28) Torrent, M.; Musaev, D. G.; Morokuma, K. *J. Phys. Chem. B* **1999**, *103*, 8618.

(29) Elmi, F.; Hadipour, N. L. *J. Phys. Chem. A* **2005**, *109*, 1729.

(30) Amini, S. K.; Hadipour, N. L.; Elmi, F. *Chem. Phys. Lett.* **2004**, *391*, 95.

(31) Frisch, M. J.; Trucks, G. W.; Schlegel, H. B.; Scuseria, G. E.; Robb, M. A.; Cheeseman, J. R.; Zakrzewski, V. G.; Montgomery, G. A., Jr.; Stratmann, R. E.; Burant, J. C.; Dapprich, S.; Millam, J. M.; Daniels, A. D.; Kudin, K. N.; Strain, M. C.; Farkas, O.; Tomsai, J.; Barone, V.; Cossi, M.; Cammi, R.; Mennucci, B.; Pomelli, C.; Adamo, C.; Clifford, S.; Ochterski, j.; Petersson, G. A.; Ayala, P. Y.; Cui, Q.; Morokuma, K.; Malick, D. K.; Rabuck, A. D.; Raghavachari, K.; Foresman, J. B.; Cioslowski, J.; Ortiz, J. V.; Stefanov, B. B.; Liu, G.; Liashenko, A.; Piskorz, P.; Komaromi, I.; Comperts, R.; Martin, R. L.; Fox, D. J.; Keith, T.; Al-Laham, M. A.; Peng, C. Y.; Nanayakkara, A.; Gonzalez, C.; Challacombe, M.; Gill, P. M. W.; Johnson, B. G.; Chen, W.; Wong, M. W.; Andres, J. L.; Head-Gordon, M.; Replogle, E. S.; Pople, J. A. *Gaussian 98*, Revision A.7; Gaussian, Inc.: Pittsburgh, PA, 1998.

(32) Becke, A. D. *J. Chem. Phys.* **1993**, *98*, 5648.

(33) Lee, C.; Yang, W. and Parr, R. G. *Phys. Rev. B* **1988**, *37*, 785.

(34) Perdew, J. P.; Wang, Y. *Phys. Rev. B* **1992**, *45*, 13244.

(35) Brender, J. R.; Taylor, D. M.; Ramamoothy, A. *J. Am. Chem. Soc.* **2001**, *123*, 914.

(36) Czernek, J. *J. Phys. Chem. A* **2001**, *105*, 1357.

(37) Wolinski, K.; Hinton, J. F. and Pulay, P. *J. Am. Chem. Soc.* **1990**, *112*, 8251.

(38) Jameson, C. J.; Mason, J. In *Multinuclear NMR*; Mason, J., Ed.; Plenum Press: New York, 1987; p 56.

(39) Pyykkö, P. *Mol. Phys.* **2001**, *99* (19), 1617.

(40) Wu, G.; Yamada, K. *Solid State Nucl. Magn. Reson.* **2003**, *24*, 196.

(41) Wu, G.; Dong, S.; Ida, R. *Chem. Commun.* **2001**, 891.

(42) Yamad, K.; Dong, S.; Wu, G. *J. Am. Chem. Soc.* **2000**, *122*, 11602.

(43) Wu, G.; Yamada, K.; Dong, S.; Grondey, H. *J. Am. Chem. Soc.* **2000**, *122*, 4215.